Talanta 84 (2011) 1390–1395

Contents lists available at ScienceDirect

Talanta

journal homepage: www.elsevier.com/locate/talanta

AAO–CNTs electrode on microfluidic flow injection system for rapid iodide sensing

Ditsayut Phokharatkul[a], Chanpen Karuwan[a,b,c], Tanom Lomas[a], Duangjai Nacapricha[b,c], Anurat Wisitsoraat[a], Adisorn Tuantranont[a,*]

[a] Nanoelectronics and MEMS Laboratory, National Electronics and Computer Technology Center, Pathumthani 12120, Thailand
[b] Flow Innovation-Research for Science and Technology (FIRST) Laboratories, Faculty of Science, Mahidol University, Rama 6 Road, Bangkok 10400, Thailand
[c] Department of Chemistry, Center of Excellence for Innovation in Chemistry, Faculty of Science, Rama 6 Road, Bangkok 10400, Thailand

ARTICLE INFO

Article history:
Available online 28 April 2011

Keywords:
Flow injection
Microfluidic device
Carbon nanotubes
Iodide detection
In-channel electrochemical detection
Lab-on-a-chip

ABSTRACT

In this work, carbon nanotubes (CNTs) nanoarrays in anodized aluminum oxide (AAO–CNTs) nanopore is integrated on a microfluidic flow injection system for in-channel electrochemical detection of iodide. The device was fabricated from PDMS (polydimethylsiloxane) microchannel bonded on glass substrates that contains three-electrode electrochemical system, including AAO–CNTs as a working electrode, silver as a reference electrode and platinum as an auxiliary electrode. Aluminum, stainless steel catalyst, silver and platinum layers were sputtered on the glass substrate through shadow masks. Aluminum layer was then anodized by two-step anodization process to form nanopore template. CNTs were then grown in AAO template by thermal chemical vapor deposition. The amperometric detection of iodide was performed in 500-μm-wide and 100-μm-deep microchannels on the microfluidic chip. The influences of flow rate, injection volume and detection potential on the current response were optimized. From experimental results, AAO–CNTs electrode on chip offers higher sensitivity and wider dynamic range than CNTs electrode with no AAO template.

1. Introduction

Microfluidics is a potential technology for biochemical processing and analysis because of low sample/reagent consumption, high sample throughput and total analysis capability [1,2]. Plastic/glass based microfluidic platforms have been extensively used for various applications due to wide functionality, low cost and disposability [3–7]. Polydimethylsiloxane (PDMS) has become a primary plastic material for miniaturized analytical system due to its high chemical and mechanical stability and a variety of PDMS based microfluidic chips [6,7] have been fabricated by standard micromolding technology [8,9].

Integration of efficient sensors or detection devices in microfluidic chips has been an important issue in the development of full functional microfluidic systems. Among a variety of detection methods, electrochemical technique is highly promising because it offers high performance detection and can directly be fabricated on plastic/glass based microfluidic chips [10]. Recently, electrochemical detection has been embedded in microfluidic systems based on end-channel [11,12] and in-channel [10,13,14] detection scheme using different electrode materials, including gold, platinum and carbon paste. Nevertheless, conventional electrochemical electrodes are not fast and highly sensitive enough for general micro total analysis applications, which involve small analyte volume and short sampling time.

Therefore, novel sensing materials should be integrated in microfluidic system to improve detection performances. Carbon nanotubes (CNTs) are promising for electrochemical sensing due to its high reaction area and excellent electron transfer rate [15]. CNTs have been widely applied as sensors in various electroanalysis applications [16–21]. Recently, microfluidic glass chips with directly grown CNTs electrode for sensitive and rapid salbutamol sensing have been reported [22]. However, naturally grown CNTs are still not yet ideal electrochemical sensors because its very high density hinders dynamics of electrochemical process. Thus, the use of CNTs for electrochemical sensing can be more effective if CNTs can be formed with micro/nano array configuration.

Anodized aluminum oxide (AAO) is a highly useful nanopore template for nanostructure formation and organization due to its low cost, ease of fabrication and high chemical stability. AAO nanopore can be used to separate CNT forest into nano array [23–26] to improve the performance of CNTs electrode by hemispherical solute diffusional effect [27]. However, there has been no report on the use of AAO–CNTs electrode in microfluidic devices.

* Corresponding author. Tel.: +66 2 564 6900; fax: +66 2 564 6771.
E-mail addresses: anurat.wisitsoraat@nectec.or.th (A. Wisitsoraat), adisorn.tuantranont@nectec.or.th (A. Tuantranont).

0039-9140/$ – see front matter © 2011 Elsevier B.V. All rights reserved.
doi:10.1016/j.talanta.2011.03.071

In this work, a new microfluidic device is developed using PDMS/glass chip with in-channel amperometric detection based on AAO–CNTs electrode. The three-electrode system was fabricated on glass substrate as an in-channel detection using thin-film sputtering and chemical vapor deposition (CVD) technique. The system was applied for determination of potassium iodide (KI). Iodide detection is of interest because it is used to determine iodide deficiency in human, which results in diseases including hypothyrodism, spontaneous abortion and cretinism. The new device would allow fast and sensitive detection of iodide with relatively low sample/reagent consumption.

2. Experimental

2.1. Chemicals and reagents

All of chemicals used in this work were analytical grade. Standard solutions of KI were purchased from Sigma (USA). Sodium phosphate monobasic monohydrate and sodium phosphate dibasic were also purchased from Sigma (USA) to prepare a phosphate buffer solution. The standard stock solution (100 mol l^{-1}) of KI was prepared by dissolving required amount of KI in the phosphate buffer solution (pH 5.8). KI solutions with different concentrations were then prepared for testing by proper dilution of the stock solution. Glass substrates, PDMS and Photoresist (SU-8 2100) were acquired from Sperior (Germany), Dow Chemical (USA), Micro Chem (USA), respectively.

2.2. Apparatus

A potentiostat, μ-autolab Type III (Metrohm, Switzerland) was used for all the cyclic voltammetric (CV) and amperometric studies. Spin coater (Laurell Technologies Corp., model WS-400A-6NPP) was used for spin coating of photoresist for mold fabrication. The MJB4 mask aligner (SUSS Microtec, Germany) was used for UV-lithography process to obtain photoresist patterns on Si-substrate. The oxygen plasma cleaner (Harrick Scientific Corp., model PDC-32G) was used for treatment of PDMS and glass surface to obtain good bonding.

2.3. Electrochemical cell for cyclic voltammetry

Cyclic voltammetry (CV) is an initial technique for characterization of electrochemical behaviors of electrodes and analytes. For CV measurement, AAO–CNTs and CNTs electrodes were fabricated on ⟨1 0 0⟩ Si substrates. The schematic structure of AAO–CNTs is illustrated in the inset of Fig. 1. First, Al (200 nm) layer was sputtered on the substrate as a contact layer and very thin layer of alumina (10 nm) was successively deposited by reactive RF sputtering. The alumina layer was used to support stainless steel catalyst (5 nm), which was subsequently sputtered on it for CNTs growth. Next, 2 μm thick Al layer was sputtered on the stainless steel catalyst. The alumina layer was deposited by reactive RF sputtering at a pressure of 3×10^{-3} mbar with 1:5 Ar:O_2 gas mixture while other metallic layers were deposited by pure Ar gas at the same pressure.

The top aluminum layer was then anodized in a 0.3 M oxalic acid solution at a constant applied voltage of 40 V for 5 min at room temperature. Next, the resultant aluminum oxide film was removed by a mixed solution of phosphoric acid (4 wt.%) and chromic acid (1.5 wt.%). The second anodization was then performed for 15 min under the same condition. The aluminum oxide layer was etched again by the etching solution for 30 min in order to widen the nanopore and expose the stainless steel catalyst.

CNTs were then grown in AAO template on silicon wafer by chemical vapor deposition (CVD) [19–21]. The CVD process is used because of its low cost and high quality CNTs structure. The catalyst

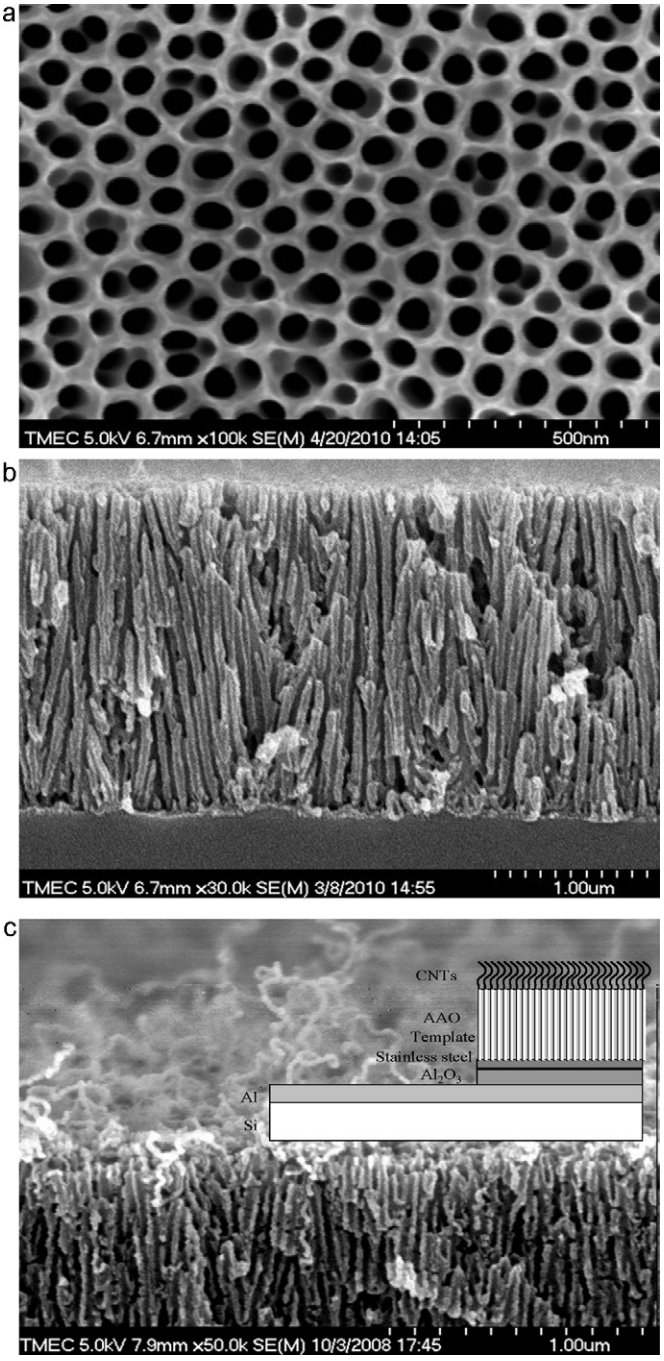

Fig. 1. SEM images of (a) top view of AAO template, (b) cross-sectional view of AAO template and (c) cross-sectional view of AAO–CNTs electrode. Inset: structure of AAO–CNTs electrode.

layer on substrates was placed on an alumina carrier in a horizontal furnace thermal CVD system. The CNTs synthesis was conducted at the atmospheric pressure and growth temperature of 700 °C. During CNTs growth, acetylene was flowed for 1.5 min and hydrogen to acetylene flow rate ratio was 4.3:1. In the course of CNTs growth, in situ water-assisted etching was employed to remove undesired amorphous carbon formation from random acetylene decomposition [21]. In water etching process, 300 ppm of water vapor was introduced by water bubbling through Ar gas for 3 min while acetylene gas was turned off. CNTs growth and water-assisted etching were repeatedly performed for five cycles.

CV experiments were performed using AAO–CNTs and CNTs electrodes in a home-made electrochemical cell. The three-

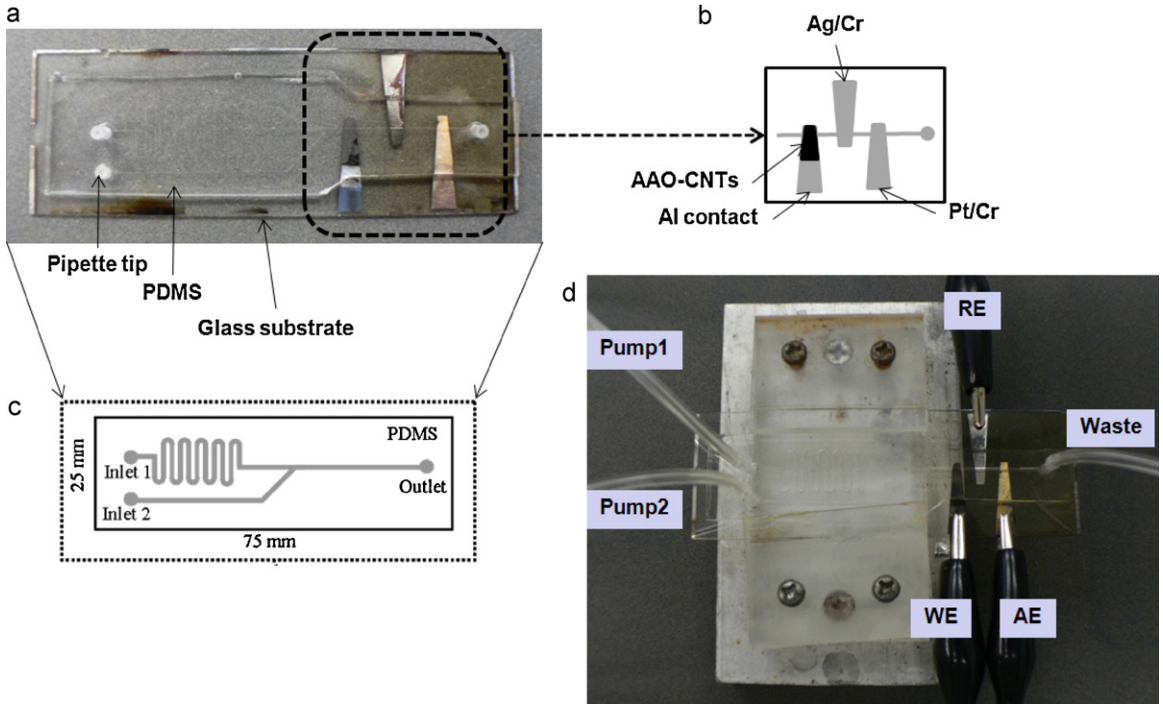

Fig. 2. Microchip and AAO–CNTs in-channel amperometric detector.

electrode system consisted of Pt wire auxiliary electrode, silver/silver chloride (Ag/AgCl) reference electrode and AAO–CNTs or CNTs working electrode. The area of working electrode was set at 0.7 cm^2 and the cell volume was 1.5 ml.

2.4. Fabrication of the miniaturized microfluidic system

The fabrication process of the miniaturized microfluidic system consisted of three main tasks. Firstly, PDMS chip containing microchannel was made by micromolding and casting process. Secondly, three-electrode system was formed on a glass substrate by sputtering and chemical vapor deposition (CVD) processes. The PDMS and glass chip were then bonded using oxygen plasma treatment. Fig. 2 shows the structure of microfluidic device with AAO–CNTs electrode.

For the fabrication of PDMS chip, microfluidic channels were fabricated based on standard photolithography. SU-8 photoresist was spun on Si substrate using spin coater and then soft baked to remove solvent in the layer. UV-lithography was performed to obtain photoresist patterns on Si substrate using MJB4 mask aligner and then post-baked in order to selectively cross-link the exposed portion of photoresist. Finally, the photoresist was developed and cleaned with deionized water and isopropyl alcohol. The microfluidic chip was designed to have two microchannel inlets and one microchannel outlet as shown in Fig. 2(c). For two microchannel inlets, one was used for buffer carrier stream and the other was for injection of analyte. The microchannel is 100 μm deep and 500 μm wide.

In the second part, three electrodes including CNTs, Pt and Ag electrodes were designed as straight stripes across microchannel as shown in Fig. 2(a) and (b). Three electrodes were located opposite to the outlet of microchannel. The auxiliary and reference electrodes were 200 μm wide and 300 nm thick platinum and silver layers each supported by 50 nm Cr adhesive layers. To obtain the AAO–CNTs working electrode, multilayer films were sputtered, top Al layer was anodized by two-step anodization process and CNTs were grown by CVD technique as previously described in Section 2.3, but in this case glass substrate was used and CNTs growth was performed at a lower temperature of 550 °C.

In the last part, the PDMS and glass chip were treated in 35-W radio-frequency oxygen plasma for 30 s. They were immediately aligned and attached after oxygen plasma treatment as shown in Fig. 2(a). Next, the inlet and outlet of microchannel were drilled and connected to micro tubing via pipette tips, which could be sealed to PDMS holes by physical attachment without the use of adhesive as shown in Fig. 2(d). The inlets were connected to syringe pumps and outlet was connected to a reservoir. Syringe pump (Pump 1) was used for propelling the running buffer into microchannel inlet 1. Microchannel inlet 2 was used for analyte injection controlled by the second syringe pump (Pump 2). Finally, the whole apparatus was mounted on an aluminum fixture and electrodes were electrically connected to potentiostat. The developed system was used for all amperometric experiments.

2.5. Microfluidic procedure

Before use, the channel was treated with deionized water for 10 min. The running buffer was PBS buffer (pH 5.8). The chronoamperograms were recorded with time while applying a detection potential at +0.6 V versus Ag/AgCl reference electrode. Sample injections were performed after stabilization of baseline buffer signal. The running buffer was delivered into the channel using a syringe pump at a controlled flow rate. The analytes were injected into the channel by propelling of syringe pump with a controlled volume.

3. Results and discussion

3.1. AAO–CNTs electrode

The device structure was characterized by scanning electron microscope (SEM). Fig. 1(a) shows the top-view SEM image of AAO template after two-step anodization. It is seen that the pore size is quite uniform and the average pore diameter is about 50 nm.

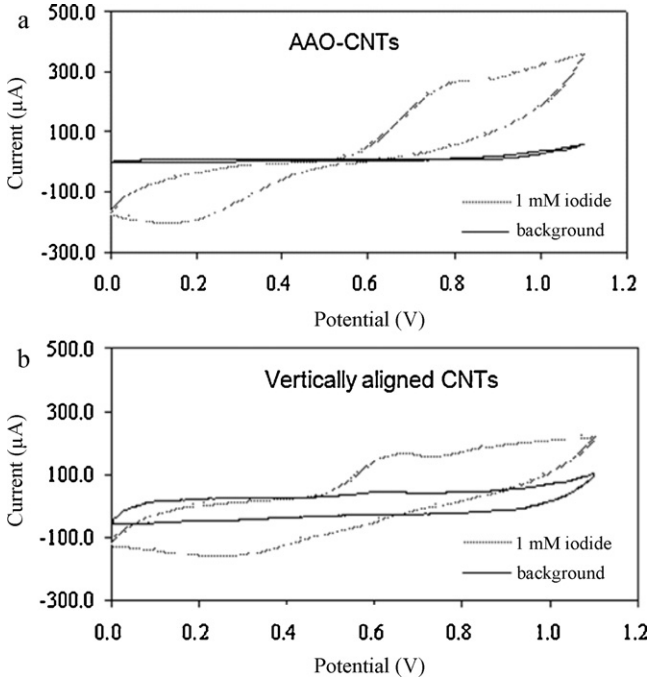

Fig. 3. Cyclic voltamograms for 1 mM iodide of (a) AAO–CNTs and (b) vertically aligned CNTs electrode in phosphate buffer solution pH 5.8.

Fig. 1(b) shows the cross-sectional view SEM image of AAO template. It is seen that the thickness of AAO layer is approximately 2 μm. Fig. 1(c) demonstrates the cross-sectional view SEM image of AAO–CNTs electrode along with its structural diagram. It can be observed that CNTs is protruded from the bottom of AAO template. The average diameter of CNTs is found to be around 30 nm by transmission microscope.

3.2. Cyclic voltammetry

In order to assess the efficacy of AAO–CNTs electrode, the electrochemical characteristics of AAO–CNTs electrode was compared to vertically aligned CNTs electrode with no AAO template. Fig. 3(a) and (b) shows cyclic voltammogram for 1 mM iodide solution of AAO–CNTs and CNTs electrodes, respectively. It is evident that AAO–CNTs electrode has much lower background current than CNTs electrode does. In addition, AAO–CNTs electrode exhibits much higher irreversible oxidation peak than vertically aligned CNTs electrode does. Thus, AAO nanopores considerably enhance the iodide response and signal to background ratio of CNTs electrode. The enhancement can be attributed to the formation of CNTs nanoarray by AAO nanopore template. The sensing area is increased and hemispherical solute diffusional effect is exploited.

Moreover, it can be noticed that there is a considerable difference between iodide peak potentials of AAO–CNTs (0.76 V in Fig. 5(a)) and CNTs (0.64 V in Fig. 5(b)) electrodes. A possible explanation for this result is that the electrical resistance of AAO–CNTs electrode is higher than that of CNTs one and it causes the observed potential shift. To validate this assumption, the resistances between electrode surface and metal contact were measured and the resistances of AAO–CNTs and CNTs electrodes were found to be ~200 Ω and ~3 Ω, respectively. The relatively high resistance of AAO–CNTs electrode can cause a potential drop of ~0.1 V when a peak current of 300 μA flows through. Thus, the assumption is highly probable. The higher resistance could be due to considerably lower density and shorter length of CNTs grown in AAO nanopores compared to CNTs grown with no AAO template.

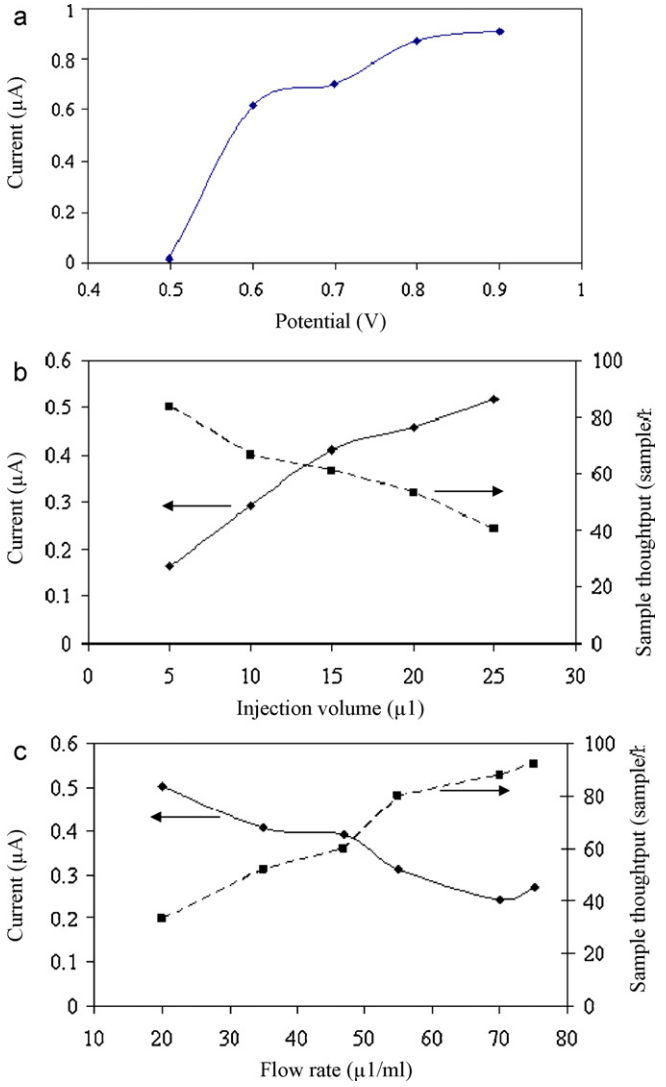

Fig. 4. Effects of (a) detection potential on current signal, (b) injection volume and (c) flow rate on current signal and sample throughput.

3.3. Flow injection optimization

The detection potential strongly affects the sensitivity of current signal of an analyte. To obtain the optimal detection potential, the hydrodynamic voltammogram was determined. Hydrodynamic voltammetry was studied from injection of 10 μl of 1 mM standard iodide solution into the micro flow system with varying detection potential from 0.5 to 0.9 V as shown in Fig. 4(a). It can be seen that the current response increases as the potential increases and seems to saturate at potential above 0.8 V. Thus, the detection potential of 0.8 V was selected for all amperometric detection in micro flow experiments.

The effect of injection volume on analytical performances of AAO–CNTs electrode was investigated over the range between 5 and 25 μl. Fig. 4(b) shows the current response and throughput versus injection volume of 1 mM standard iodide at a fixed flow rate of 50 μl/min. It is evident that throughput decreases but current signal increases with increasing injection volume. The injection volume of 15 μl was thus chosen to compromise sensitivity and throughput (60 samples/h).

In order to achieve the satisfactory sensitivity and sample throughput, the effect of flow rate was optimized using the injection of 15 μl of standard iodide solution. Fig. 4(c) shows that the

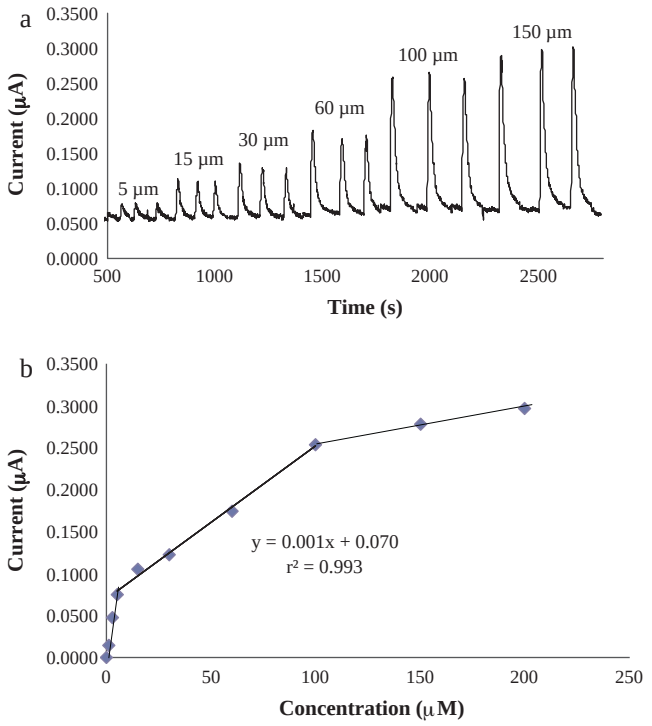

Fig. 5. (a) Effects of concentration of standard iodide on current signal and (b) calibration curve.

response decreases with increasing flow rate from 20 to 75 μl/min. Conversely, increasing flow rate increases sample throughput. To balance between response and sample throughput, the flow rate of 50 μl/min was selected.

3.4. Microfluidic system with amperometric detection

In order to test fouling or adsorption of the analyte compound on AAO–CNTs electrode, responses from replicate injections of standard iodide of 1 mM were evaluated in term of relative standard deviation (RSD). The developed system gave a fair repeatability with RSD of 8.86% (n = 12) so fouling of the AAO–CNTs electrode was considered low. However, the result was still not acceptable and it should be improved by further optimizing electrode structure as well as conditions for amperometric detection.

In order to obtain a calibration curve, the varied concentrations of standard iodide from 1 to 200 μM were injected into the system and current response amplitude was measured. Fig. 5(a) shows the effect of concentration on current signal with different concentrations ranging from 1 to 200 μM with three replicate injections. Fig. 5(b) demonstrates the calibration curve of current signal over concentration ranging from 1 to 200 μM. It can be seen that linear concentration dependence is observed in the range between 5 and 100 μM. The regression equation is given by $y = 0.001x + 0.07$ (r^2 = 0.993), where y and x are the height of peak current (μA) and iodide concentration (μM), respectively. The slope of the equation is corresponding to linear sensitivity of 0.001 μA/μM. The detection limit (3S/N) is ~0.5 μM. At low concentration (less than 5 μM), iodide peak current also varies linearly but with a higher slope value. On the other hand, the response current begins to level off at higher iodide concentrations (100–200 μM).

3.5. Real sample analysis and interference study

The possibility for the use of the developed system in real sample analysis was studied with pharmaceutical products containing iodide. Iodide contents in four pharmaceutical tablets, namely 'Centrum', 'Bioton', 'Obimin' and 'Revicon' were analyzed by the developed electrochemical system. Tablets were ground before extraction with water, centrifuged and filtrated through 0.25 μm cellulose acetate membrane. The filtrates were then suitably diluted with 50 mM tris buffer pH 5.8. The measured results were compared to the labeled values from their manufacturer and results from ion selective electrode (ISE) potentiometric analysis as shown in Table 1. ISE measurement was conducted by a commercial digital Orion ion-analyzer (model 601A). Before ISE measurement, the ion strength of solution was adjusted by adding suitable amount of 5 M $NaNO_3$ solution. The potential developed across the employed iodide-ISE (Orion, USA) and the saturated calomel electrode (Orion) was then measured in the prepared sample solution.

It can be seen that the results for Obimin and Revicon from our developed system are in fair agreement to those obtained from standard ISE method. The results determined by both methods are considered not greatly different at 95% confidence by paired t-test (t_{stat} = 0.85, $t_{critical}$ = 2.57). However, the differences between the results from our and standard method are quite notable (10–20%). Thus, there is considerable interference to iodide by other species in Obimin and Revicon. In addition, it was found that very strong interference occurred in other tested products including Centrum and Bioton.

Further interference study was conducted to identify species that contribute strong interference. Interferences were tested towards three electroactive species including ascorbic acid, chloride and bromide, which were major ingredients in these pharmaceutical tablets, at their nominal concentrations. Table 2 summarizes the interference results of ascorbic acid (40–320 mg/dl), chloride (40–160 mg/dl) and bromide (40–200 mg/dl) in 90 μM potassium iodide solution. It can be seen that chloride and bromide give very low interference signals while ascorbic acid produces considerable interference. Thus, ascorbic acid, which is an active ingredient of Revicon, is one of strong interference species that

Table 1
Comparison of the labeled values of iodide content in pharmaceutical products and the analyzed results by ISE analysis and flow injection chronoamperometry using AAO–CNTs electrode.

Samples	Content of iodide (μg/tablet)		
	Label	AAO–CNTs electrode	Ion selective electrode
Revicon 1	200	220 ± 12	195 ± 7.2
Revicon 2	200	226 ± 9.3	197 ± 5.2
Revicon 3	200	227 ± 7.1	198 ± 4.5
Obimin 1	100	80 ± 4.7	98 ± 5.3
Obimin 2	100	86 ± 5.6	96 ± 4.6
Obimin 3	100	86 ± 3.3	97 ± 4.3

Table 2
Effects of foreign ions on the current signal obtained from adding of foreign species into 90 μM potassium iodide solution.

Foreign species	Content label in some sample (mg/l)	Results[a]
Vitamin C or L(+)ascorbic acid/$C_8H_8O_6$	90–100	Strongly interfere (studied from 40 to 320 mg/l)
Cl^-/NaCl	40	Does not interfere (studied from 40 to 160 mg/l)
Br^-/NaBr	40	Does not interfere (studied from 40 to 200 mg/l)

[a] Greater than ±5% signal variation is classified as interfering condition.

should be separated to avoid analysis errors. From these results, AAO–CNTs electrode does not possess general anti-interference capability. Sample pretreatment including separation is needed to overcome the interference problem in general cases especially urine samples, which contain very complex matrices.

4. Conclusions

In conclusion, in-channel amperometric microfluidic device with AAO–CNTs electrode has successfully been developed for iodide detection. The device demonstrates the first utilization of AAO–CNTs electrode on glass based microfluidic chip for iodide detection. The electrocatalytic activity of iodide on AAO–CNTs is good when compared with vertically aligned CNTs electrode with higher response and signal to background ratio. Moreover, AAO–CNTs electrode exhibits good stability in flowing system and fair reproducibility for amperometric detection. Thus, the combination of sensitive AAO–CNTs electrode and miniaturized analysis system is a new and promising technique for chemical detection.

Acknowledgements

The authors would like to acknowledge the research funding from National Electronics and Computer Technology Center and National Science and Technology Development Agency. Adisorn Tuantranont would like to express his gratitude for Researcher Career Development Grant from Thailand Research Fund (TRF). And from the Center for Innovation in Chemistry: Postgraduate Education and Research Program in Chemistry (PERCH-CIC).

References

[1] H. Becker, L.E. Locascio, Talanta 56 (2002) 267–287.
[2] D.R. Rwyes, D. Iossifidis, P.A. Auroux, A. Manz, Anal. Chem. 74 (2002) 2623–2636.
[3] Y. Liu, D. Ganser, A. Schneider, R. Liu, P. Grdzinski, N. Kroutchinina, Anal. Chem. 73 (2001) 4196–4201.
[4] S.M. Ford, B. Kar, S. McWhorter, J. Davies, S.A. Soper, M. Klopf, G. Calderon, V.J. Saile, Microcolumn 10 (1998) 413–422.
[5] J.C. McDonald, D.C. Duffy, J.R. Anderson, D.T. Chiu, H. Wu, O.J.A. Schueller, G.M. Whitesides, Electrophoresis 21 (2000) 27–40.
[6] M.J. Schoning, M. Jacobs, A. Muck, D.-T. Knobbe, J. Wang, M. Chatrathi, S. Spillmamm, Sens. Actuators B 108 (2005) 688–694.
[7] O. Yassine, P. Morin, O. Dispagne, L. Renaud, L. Denoroy, P. Kleimann, K. Faure, J.-L. Rocca, N. Ouaini, R. Ferrigno, Anal. Chim. Acta 609 (2008) 215–222.
[8] G.S. Virdi, R.K. Chutani, P.K. Rao, S. Kumar, Sens. Actuators B 128 (2008) 422–426.
[9] Micro Chem, Nano SU-8 2000, Negative Tone Photoresis Formulations 2035–2100.
[10] K.-W. Lin, Y.-K. Huang, H.-L. Su, Y.-Z. Hsieh, Anal. Chim. Acta 619 (2008) 115–121.
[11] M. Castano-Alvarez, M.T. Fernansez-Abedul, A. Costa-Garcia, J. Chromotogr. A 1109 (2006) 291–299.
[12] D.F. Pozo-Ayuso, M. Castano-Alvarez, A. Fernansez-la-Villa, M. Garcia-Granda, M.T. Fernandez-Abedul, A. Costa-Garcia, J. Rodriguez-Garcia, J. Chromotogr. A 1180 (2008) 193–202.
[13] K.-T. Liao, C.-M. Chen, H.-J. Huang, C.-H. Lina, J. Chromotogr. A 1165 (2007) 213–218.
[14] N. Dossi, R. Toniolo, A. Pizzariwllo, S. Susmel, F. Perennes, G. Bontempelli, J. Electroanal. Chem. 601 (2007) 1–7.
[15] S. Shahrokhian, H.R. Zare-Mehrjardi, Electrochim. Acta 52 (2007) 6310–6317.
[16] S. Roy, H. Vedala, W. Choi, Nanotechnology 17 (2006) S14–S18.
[17] J.-E. Huang, X. Hong, H.-L. Li, Carbon 41 (2003) 2731–2736.
[18] A. Wisitsoraat, A. Tuantranont, E. Comini, G. Sberveglieri, W. Wlodarski, IEEE Sensors 2007 Conf., October 28–31, 2007, IEE Sensors, 2007, pp. 550–553.
[19] Y. Wanna, N. Srisukhumbowornchai, A. Tuantranont, A. Wisitsoraat, N. Thavaungkul, P. Singjai, J. Nanosci. Nanotechnol. 6 (2006) 3893–3896.
[20] A. Wisitsoraat, A. Tuantranont, C. Thanachayanont, V. Patthanasettakul, P. Singjai, J. Electroceram. 17 (2006) 45–49.
[21] S. Chaisitsak, J. Nukeaw, A. Tuantranont, Diam. Relat. Mater. 16 (2007) 1958–1966.
[22] C. Karuwan, A. Wisitsoraat, T. Maturos, D. Phokharatkul, A. Sappat, K. Jaruwongrungsee, T. Lomas, A. Tuantranont, Talanta 79 (2009) 995–1000.
[23] J.S. Lee, G.H. Gu, H. Kim, K.S. Jeong, J. Bae, J.S. Suh, Chem. Mater. 13 (2001) 2387–2391.
[24] S.Y. Jeong, M.C. An, Y.S. Cho, D.J. Kim, M.C. Peak, K.Y. Kang, Curr. Appl. Phys. 9 (2009) S101–S103.
[25] H. Masuda, H. Yamada, M. Satoh, H. Asoh, Appl. Phys. Lett. 71 (1997) 2770–2772.
[26] M. Tian, S. Xu, J. Wang, N. Kumar, E. Wertz, Q. Li, P.M. Campbell, M.H.W. Chan, T.E. Mallouk, Nano Lett. 5 (2005) 697–703.
[27] M.-H. Spyridaki, P. Kiousi, A. Vonaparti, P. Valavani, V. Zonaras, M. Zahariou, E. Sianos, G. Tsoupras, C. Georgakopoulos, Anal. Chim. Acta 573 (2006) 242.